An Assessment of Radiation Effects in Beryllium

W.G. Wolfer and T.J. McCarville

February 1985

UWFDM-632

Presented at the Sixth Topical Meeting on the Technology of Fusion Energy, San Francisco, CA, 3-7 March 1985; Fusion Tech. 8, (July 1985).

FUSION TECHNOLOGY INSTITUTE

UNIVERSITY OF WISCONSIN

MADISON WISCONSIN

An Assessment of Radiation Effects in Beryllium

W.G. Wolfer and T.J. McCarville

Fusion Technology Institute
University of Wisconsin
1500 Engineering Drive
Madison, WI 53706

http://fti.neep.wisc.edu

February 1985

UWFDM-632

Presented at the Sixth Topical Meeting on the Technology of Fusion Energy, San Francisco, CA, 3-7 March 1985; Fusion Tech. 8, (July 1985).

AN ASSESSMENT OF RADIATION EFFECTS IN BERYLLIUM

W.G. WOLFER
Department of Nuclear Engineering
University of Wisconsin, Madison, WI 53706
(608) 263-3368

T.J. MCCARVILLE
TRW Energy Development Group
Redondo Beach, CA 90278
(213) 539-9241

ABSTRACT

Radiation effects in beryllium as produced by fast neutrons and resulting in dimensional changes are reviewed. It is found that helium bubble swelling is the predominant mechanism; however, because of the intrinsic anisotropy of the dislocation structure, bubble swelling is expected to be anisotropic, accompanied by radiation-induced growth. The anisotropy of swelling and plastic deformation at the microscopic level of crystal grains eventually results in microcracking, and the total inelastic deformation should therefore not exceed about 1%.

1. INTRODUCTION

Beryllium and graphite are two leading candidate materials for limiters and other high heat flux components in immediate contact with the plasma. Recent experiments on the ISX-B device with a beryllium limiter demonstrated the suitability of this material,[1] and it is therefore also being considered for use in other near-term fusion devices. For these devices, the major advantages of beryllium are the low Bremsstrahlung losses as an impurity in the plasma, and the absence of chemical sputtering. However, for future fusion reactors, radiation damage is a cause of concern.

It is therefore the main purpose of this paper to present a discussion of the radiation effects issues and to assess the magnitude and severity of the various radiation effects. Although many aspects of this assessment will turn out to be somewhat speculative for lack of information on basic physical parameters, it will nevertheless be possible to clearly identify and quantify the major radiation effect in beryllium, namely the formation of helium bubbles and the associated swelling. Since beryllium is an anisotropic metal with a hexagonal closed-packed crystal structure, other components of dimensional changes can be produced by neutron irradiation. In fact the complete list of radiation-induced deformations to be discussed is as follows:

a) bubble swelling,
b) void swelling,
c) radiation-induced growth,
d) irradiation creep,
e) microcrack formation.

The last three effects are closely related and are to a large extent determined by the anisotropy of the dislocation microstructure and the anisotropy of diffusion. The relative importance of bubble and void swelling is controlled by the rates of helium production and displacement damage. Accordingly, as an essential prerequisite for the assessment of the above radiation effects, it will be first necessary to examine in Sections 2 and 3 the primary damage produced by 14 MeV neutrons in beryllium. Second, the basic properties of interstitials and vacancies are discussed in Section 4. With these fundamental properties it is then possible to estimate the helium-induced swelling in Section 5. In Section 6 we assess the possibility for void swelling and radiation-induced growth. The last two sections are devoted to a short discussion of irradiation creep and microcracking.

2. HELIUM PRODUCTION

The neutron cross sections responsible for the helium production[2] in beryllium are shown in Fig. 1. The most prominent inelastic nuclear reaction above a threshold energy of 2.7 MeV is the (n,2n) reaction

$$^{9}_{4}\mathrm{Be} + n \rightarrow {}^{8}_{4}\mathrm{Be} + 2n \ ,$$

with the subsequent decay of half-life 2×10^{-15} s to

$$^{8}_{4}\mathrm{Be} \rightarrow 2\ {}^{4}_{2}\mathrm{He} + 94\ \mathrm{keV} \ .$$

The kinetic energy of the two α-particles contributes a significant amount of displacement damage as will be shown below.

The second reaction of interest is the (n,α) reaction with a threshold energy of about 0.7 MeV, and it gives rise to the following se-

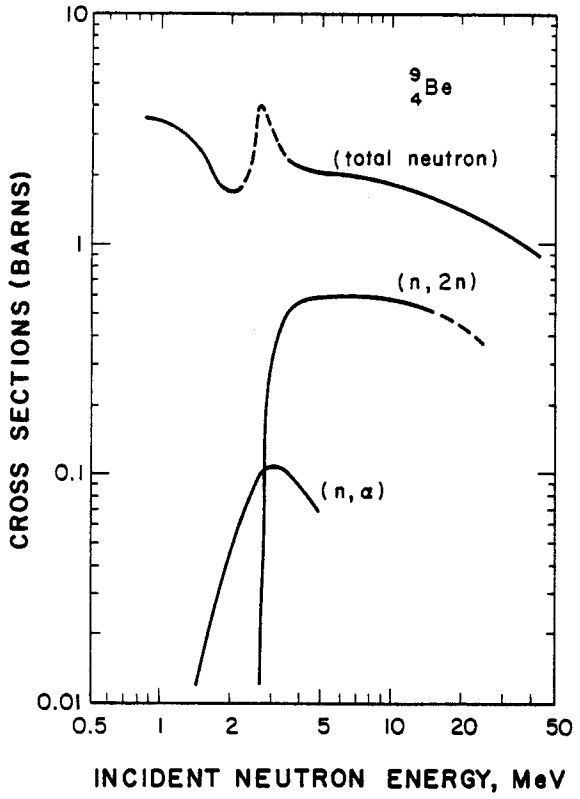

Fig. 1. Neutron cross-sections for Be.

quence:

$$^{9}_{4}Be + n \rightarrow {}^{4}_{2}He + {}^{6}_{2}He$$

$$^{6}_{2}He \xrightarrow[0.85\ s]{\beta^-} {}^{6}_{3}Li$$

$$^{6}_{3}Li + n \rightarrow {}^{4}_{2}He + {}^{3}_{1}H$$

$$^{3}_{1}H \xrightarrow[12.5\ y]{\beta^-} {}^{3}_{2}He \ .$$

Again, this reaction sequence leads to the production of two helium atoms in addition to one tritium atom. However, as Fig. 1 illustrates, the cross-section for the (n,α) reaction is probably very small in comparison with the one for the (n,2n) reaction at neutron energies of 14 MeV. Hence, when backscattering and neutron moderation can be neglected, the helium production can be adequately estimated based on the (n,2n) reaction alone. As an example, consider a neutron wall loading of 1 MW-yr/m^2 produced by a D-T plasma. The unmoderated neutron fluence is in this case 2.8 x 10^{21} n/cm^2 (E = 14.03 MeV), and it generates 2918 appm-He/yr in a beryllium structure. A more precise evaluation of the actual helium production requires the specification of the blanket geometry, its composition and other design aspects. For instance, for a thick multiplier blanket surrounding a tandem mirror hybrid reactor with a wall loading of 1 MW/m^2, Lee et al.[3] obtained the helium production profile as shown in Fig. 2. The multiplier is assumed to have slab geometry and contain a volume fraction of 53% beryllium. As a result of the significant backscattering of neutrons, the helium production rate on the plasma side is increased to about 3700 appm-He/yr.

In fission reactors, the (n,α) reaction must be taken into account when evaluating the helium production in beryllium. Beeston et al.[4] have estimated that the production rate of helium in beryllium exposed in the ATR and ETR is about 4700 appm-He per 10^{22} n/cm^2 (E > 1 MeV).

3. DISPLACEMENT PRODUCTION

The elastic scattering of 14 MeV neutrons with the beryllium atoms produces primary recoil atoms with energies up to 5.05 MeV. If we assume that the elastic scattering cross-section is to a first approximation isotropic, then the average primary recoil energy is half the maximum value, i.e. 2.53 MeV. Each primary recoil atom produces a collision cascade resulting in the following number of displacements

$$\nu_n = \xi(\bar{T}) \frac{\bar{T}}{2E_d} \ .$$

Here, $\bar{T}$ is the average recoil energy, E_d the displacement energy, and $\xi(\bar{T})$ the displacement efficiency.

The displacement energy can be estimated from empirical correlations. According to Mitchell et al.[5] the displacement energy of metals is nearly proportional to the sublimation energy; the latter, however, is also nearly proportional to the melting temperature, T_m, so that

$$E_d \cong 150\ k_B T_m$$

where k_B is the Boltzmann constant in eV. For beryllium, this empirical correlation gives a displacement energy of E_d = 19 eV.

The displacement efficiency, ξ, is defined as the fraction of the primary projectile energy which results in subsequent displacements. It has been evaluated by Robinson[6] using the Lindhard theory of electronic energy loss. When applied to beryllium, the results shown in Fig. 3 are obtained. It is seen that the very energetic recoil atoms produced by 14 MeV neutrons possess a very low damage efficiency. This is due to the fact that electronic energy losses are dominant in low Z materials. A recoil atom

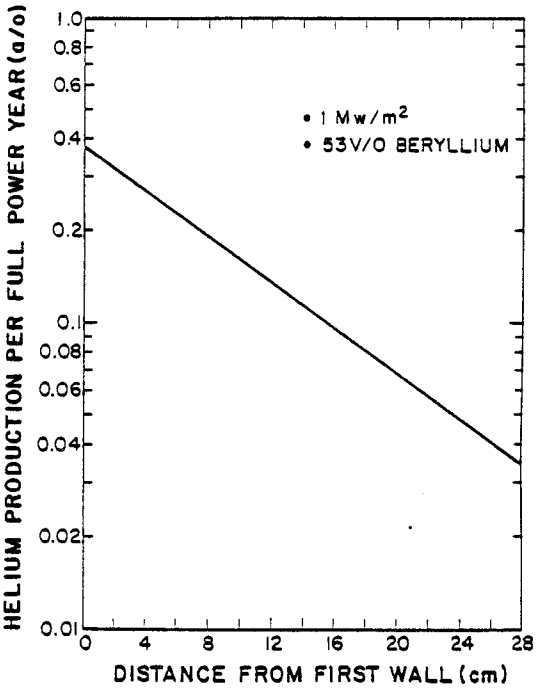

Fig. 2. Helium production in a beryllium containing blanket of a hybrid mirror reactor.

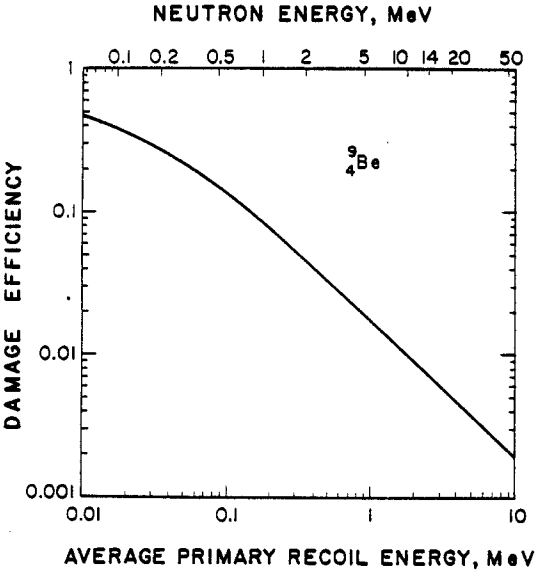

Fig. 3. Displacement damage efficiency for recoils in Be.

of average energy (2.53 MeV) produces then an average of $\nu_n \cong 480$ displacements. In contrast, primary recoil atoms generated by a 1 MeV neutron have an average energy of about 180 keV and they each produce $\nu_n \cong 384$ displacements.

The elastic scattering cross-section of 14 MeV neutrons with beryllium is, according to Fig. 1, about 1.08 barns. Therefore, a neutron fluence corresponding to 1 MW-yr/m^2 generates about 1.45 dpa in beryllium by elastic collisions alone. Additional displacement damage is created by the helium atoms which possess a primary energy of 47 keV. The displacement efficiency of these helium atoms is $\xi \cong 0.9085$, so that the total helium generated by a neutron wall loading of 1 MW/m^2 will contribute the additional amount of 3.28 dpa/yr. In total, the displacement rate produced in beryllium by a neutron wall loading of 1 MW/m^2 is equal to about 4.73 dpa/ yr, and the ratio of helium to displacement production is 617 appm-He/dpa.

To compare this with the damage produced in a fission reactor, a fluence of 10^{22} n/cm^2 of energy 1 MeV creates 12.7 dpa by elastic collisions and about 5.3 dpa as a result of the helium production, resulting in a total of 18 dpa and a ratio of helium to displacement production of 261 appm-He/dpa. To put these numbers in perspective it is noted that the ratio of helium to displacement production in type 316 stainless steel is about 0.6 appm-He/dpa in a breeder reactor and 20 appm-He/dpa in a fusion reactor. Helium bombardments of metal surfaces for the purpose of carrying out blistering studies are estimated to give a ratio of about 1000 appm-He/dpa.

4. DIFFUSION PROPERTIES

The dimensional changes which accompany radiation damage at elevated temperatures are caused by the accumulation of vacancies and interstitials in the form of cavities, dislocation loops and network dislocations. The rate of growth of these microstructural features depends to a large extent on the diffusion coefficients of self-interstitials, vacancies, and helium atoms.

Although no direct measurements have been made of the interstitial diffusion, Delaplace et al.[7] have observed a stage I recovery at about 45 K and a stage III recovery at about 280 K. The former is usually ascribed to the uncorrelated migration of the self-interstitial, whereas the latter is traditionally associated with vacancy migration. If we accept this usual assignment, then the activation energy for interstitial migration is estimated to be around 0.15 eV. This value is within the range from 0.065 to 0.2 eV found by Beeler[8] in computer simulations of interstitial migration in an ideal hcp crystal lattice. The stage III recovery at about 280 K would indicate a vacancy migration energy of about 0.82 eV.

On the other hand, measurement of the self-diffusion coefficient by Dupouy et al.[9] indicated a strong anisotropy with a self-diffusion coefficient parallel to the c-axis of

$$D_{SD}^{c} = 0.62 \exp[-1.71 \text{ eV}/k_B T] \text{ cm}^2/\text{s}$$

and perpendicular to the c-axis of

$$D_{SD}^{a} = 0.52 \exp[-1.63 \text{ eV}/k_B T] \text{ cm}^2/\text{s} .$$

The activation energies in these expressions contain the sum of the vacancy formation and migration energies, whereas the pre-exponential factors incorporate a factor $\exp[S_v^f/k_B]$, where S_v^f is the entropy for vacancy formation. Its value can be estimated from the semi-empirical expression

$$S_v^f/k_B = 1.83 + 3.4 \times 10^{15} K\alpha\Omega$$

given by Burton.[10] Here $K = 1.1158 \times 10^{12}$ dynes cm^{-2} is the bulk modulus, $\alpha \cong 1.5 \times 10^{-5}$ the linear thermal expansion coefficient, and $\Omega = 8.272 \times 10^{-24}$ cm^3 is the atomic volume. With the given numerical values for beryllium one finds $S_v^f/k_B = 2.3$ and $\exp[S_v^f/k_B] = 9.98 \cong 10$.

A separate measurement of the vacancy formation energy does not exist. However, Myers[11] has estimated its value by computer simulation to be between 0.9 and 1.0 eV. If we adopt a value of $E_v^f = 0.95$ eV, the following diffusion coefficients for vacancy migration are obtained parallel and perpendicular to the c-axis:

$$D_v^c = 0.062 \exp[-0.76 \text{ eV}/k_B T] \quad (1)$$

$$D_v^a = 0.052 \exp[-0.68 \text{ eV}/k_B T] . \quad (2)$$

The thermal equilibrium concentration of vacancies in atomic fraction is then given by

$$C_v^{eq} = 10 \exp[-0.95 \text{ eV}/k_B T] . \quad (3)$$

No measurement exists on the diffusion of helium in beryllium. However, based on diffusion in other metals, it is probably safe to assume that a helium atom once trapped in a vacancy diffuses with the vacancy, and the complex has an activation energy for migration similar to a free vacancy.

5. HELIUM BUBBLE SWELLING

The formation and growth of helium bubbles in metals can take place by both athermal and thermal processes, depending on the irradiation temperature.[12] When self-diffusion is insignificant, the growth proceeds by the emission of self-interstitials which remain trapped near the bubble, or by the punching of interstitial loops. For both cases there exists a pressure in the bubble which greatly exceeds the bubble equilibrium pressure of $2\gamma/r$, where r is the bubble radius and γ the surface energy. In fact, the helium density within the bubble remains nearly equal to the solid packing density, and swelling is simply equal to

$$\frac{\Delta V}{V_o} = \frac{V_{He}}{\Omega} C_{He} \quad (4)$$

where Ω is the atomic volume of the host metal, V_{He} is the molar volume of dissolved helium, and C_{He} is the atomic fraction of helium.

Equation (4) has been fitted to the swelling data reported by Beeston[4] for beryllium irradiated at about 100°C, with the result that

$$\frac{\Delta V}{V_o} (\%) = [0.52 \pm 0.23]\phi t , \quad (5)$$

where ϕt is in units of 10^{22} n/cm^2 ($E > 1$ MeV). Per unit of this fluence, about 0.9 at.% of helium is produced, so that Eq. (5) can also be written as

$$\frac{\Delta V}{V_o} (\%) = [0.58 \pm 0.25] C_{He}(\text{at.}\%) . \quad (6)$$

This equation implies a molar volume of helium in Be of

$$V_{He} = [0.58 \pm 0.25]\Omega$$

which is very similar to the value of 0.62 Ω obtained from computer simulation studies of helium clusters in Cu by Baskes and Holbrook.[13] Equation (6) is expected to be applicable for irradiation temperatures $\lesssim$ 250°C for which self-diffusion is negligible.

At higher temperatures self-diffusion allows bubbles to grow by absorption of thermal vacancies. In this case, the bubble pressure remains close to the equilibrium pressure

$$P = 2\gamma/r .$$

If this equation is multiplied by the bubble fractional volume then the left hand side becomes equal to $C_{He}kT$ if an ideal gas law is assumed. Since the bubble volume can also be written as $\Delta V/V_o = (4\pi/3)Nr^3$, where N is the bubble density, we obtain

$$\frac{\Delta V}{V} (\%) = 100 \left(\frac{3}{4\pi N}\right)^{1/2} \left(\frac{C_{He} kT}{2\gamma}\right)^{3/2} . \quad (7)$$

Beeston[4] has experimentally determined the bubble density in post-irradiation annealed beryllium samples. For samples irradiated at about 100°C no visible bubbles were found until the annealing temperatures exceeded 300°C, which is close to the estimated temperature where self-diffusion becomes important.

The measured bubble densities for annealing temperatures between 400°C and 600°C are given by the empirical equation

$$N = 1.4 \times 10^{14} \exp(0.41 \text{ eV}/k_B T) \text{ cm}^{-3} \quad (8)$$

The reported measurements of the surface energy γ of beryllium are 1 J/m^2,[14] and 1.6 J/m^2.[15] However, Muir[16] list a value of 2 J/m^2, which would be in better agreement with empirical correlations based upon melting temperature and cohesive energy.

Accordingly, bubble swelling predictions were made for surface energy values of 1 J/m^2 and 2 J/m^2 by using Eqs. (6) and (7). At low temperatures, Eq. (7) predicts swelling values below the values obtained with Eq. (6). Hence, it is assumed that the actual bubble swelling is determined by whichever equation provides the largest value. The results for a surface energy of 2 J/m^2 are shown in Fig. 4. Measured swelling values for the annealed samples are also indicated in these figures together with the estimated helium concentrations.

It was found that better agreement between the theoretical predictions and the measured data is obtained when a value of 2 J/m^2 is assumed for the surface energy of beryllium. It is also found that the transition temperature where equilibrium bubble swelling becomes equal to the "solid helium" swelling shifts to lower values with the increase in the helium concentration.

6. VOID SWELLING AND RADIATION-INDUCED GROWTH

A necessary condition for both void swelling and radiation-induced growth to occur is the presence of a bias. For a bias to exist there must be microstructural sinks which possess different preferences for the absorption of interstitials and vacancies.

In cubic metals it is generally the dislocations which absorb interstitials preferentially and voids receive by default a small excess of vacancies. This is then the cause of void swelling. In anisotropic solids the preference for point defect absorption may be fundamentally different from cubic metals. First, the bias of a dislocation depends on its orientation.

Woo and Goesele[16] have shown that an edge dislocation whose line direction is oriented with an angle λ to the c-axis direction has the following bias factor for vacancy absorption

$$Z_v = \left[\frac{D_v^a}{D_v^c}\cos^2\lambda + \sin^2\lambda\right]^{1/2}\left[1 - \frac{\ln f}{\ln\left(\frac{R}{r_o}\right)}\right]^{-1} \quad (9)$$

where 2R is the average distance between two

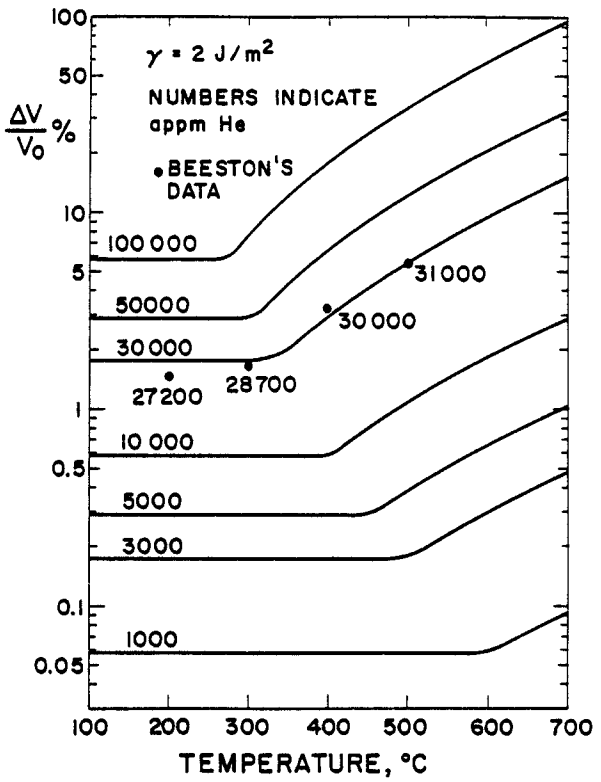

Fig. 4 Helium bubble swelling in neutron irradiated and post-irradiation annealed Be.

dislocations, r_o is the dislocation core radius,

$$f = [x^{1/2} + x^{-1/2}]^{1/2}[x^{1/4} + x^{-1/4}]_2^{-3/2} \quad (10)$$

and

$$x = \cos^2\lambda + \left(\frac{D_v^c}{D_v^a}\right)\sin^2\lambda \ . \quad (11)$$

Z_v has been evaluated for two edge dislocations, one in the basal plane ($\lambda = \pi/2$) and one perpendicular to it ($\lambda = 0$), and the results are shown in Fig. 5 as solid curves. An edge dislocation lying in the basal plane receives less vacancies than an edge dislocation oriented along the c-axis. This difference arises from the anisotropy of vacancy diffusion.

If we assume that interstitials migrate in beryllium with an activation energy of 0.1 eV parallel to the c-axis and with an activation energy 0.15 eV parallel to the basal planes then the bias factors Z_I for interstitial absorption are as shown by the dashed curves in Fig. 5. In

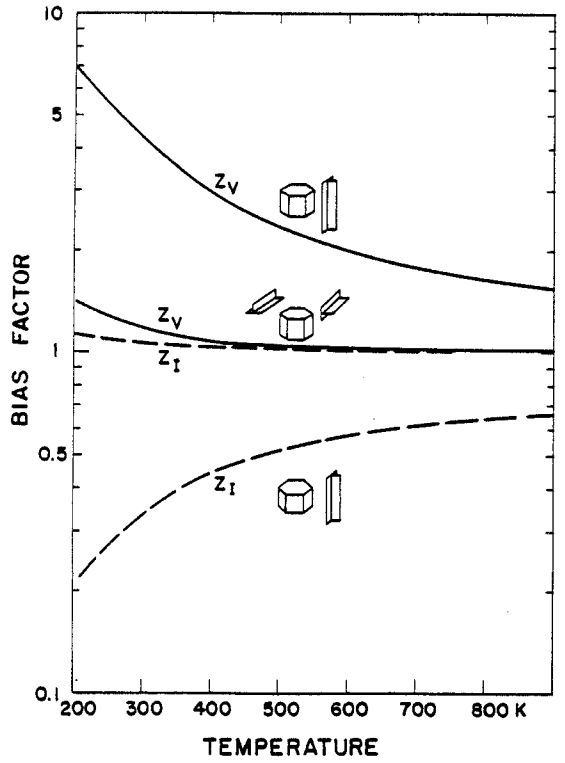

Fig. 5. The bias factors for vacancy absorption (Z_V) and interstitial absorption (Z_I) at dislocations in Be of different orientations.

this case, dislocations lying in the basal planes receive more interstitials than dislocations oriented perpendicular to the basal planes.

As a result of this preferred absorption at different dislocations, one expects that radiation induces an anisotropic shape change of the individual grains of a beryllium polycrystal. The radiation-induced growth elongates the grains in the c-direction and reduces the transverse dimension. The severity of this effect depends on the ratio of the dislocation densities with c-type Burgers vector and a-type Burgers vectors.

In unirradiated beryllium, this ratio is known to be very small. In fact the lack of c-type dislocations is believed to be the basic cause of the low ductility of beryllium.

As a result, in spite of the large differences in the bias of c-type and a-type dislocations, little radiation-induced growth is expected. This has been confirmed experimentally by Carpenter and Fleck[18] during the HVEM irradiation of beryllium and zirconium specimens. Radiation-induced growth produced a noticeable bulge in the Zr foil, but no bulge was observed in the Be foil for doses up to about 15 dpa. From the visible microstructure produced by the radiation damage, Carpenter and Fleck concluded that only one out of 10^5 defects produced in Be was retained in the microstructure.

The prevalence of a-type dislocations together with their preferred absorption of vacancies (see Fig. 5) makes void formation and growth in Be very unlikely. For this reason, and because of the high He/dpa ratio, bubble swelling is the dominant, if not the only cause of swelling in Be. However, bubble swelling is not necessarily isotropic. The metal atoms expelled from the growing gas bubble are absorbed at dislocations or form dislocation loops. It is the climbing dislocations and the growing interstitial loops which actually produce the swelling. Since this evolving dislocation structure is anisotropic, bubble swelling is expected to be accompanied by growth.

7. IRRADIATION CREEP

The mechanism of irradiation creep in non-cubic metals is unknown, and it is presently not possible to make a prediction of the enhancement of creep under irradiation. Only one measurement of irradiation creep in beryllium has been reported in the literature by Hesketh.[19] This experiment has been carried out with loaded helical springs irradiated at a temperature of 316 K in the Dounreay Materials Testing Reactor under a fast neutron flux of 1.5×10^{13} n/cm^2/s. If it is assumed that the average fast neutron energy is 1 MeV, then the displacement rate in this experiment was 1.35×10^{-8} dpa/s. The steady-state irradiation creep rate as reported by Hesketh is then given by

$$\dot{\varepsilon} = 3.2 \times 10^{-12} \sigma \ [\text{dpa}^{-1}] \qquad (12)$$

where $\dot{\varepsilon}$ is the equivalent strain rate per dpa and σ is the equivalent stress given in Pa. Since irradiation creep is only weakly dependent on temperature, Eq. (12) may serve as a crude estimate for the creep rate at all temperatures where self-diffusion is insignificant, i.e. below about 300°C. For an exposure of 10 MW-yr/m^2 and a stress of 200 MPa, an irradiation creep strain of about 0.93% is obtained. In comparison, the swelling at temperatures below 300°C is estimated to be about 1.8% for the same exposure.

8. MICROCRACKING

As a result of the great difficulty of slip in directions not parallel to basal planes, plastic deformation in beryllium polycrystals will eventually lead to residual microstresses which can only be relieved by microcracking at low temperatures, or by diffusional processes involving dislocation climb at temperatures above about 350°C.

Turner et al.[20] have investigated the occurrence of microcracking after plastic deformation at room temperature. They observed small cleavage cracks of 0.5 μm length when the tensile strain exceeded about 1%; the number of grains cleaved increased linearly with tensile strains exceeding 1%. The orientation of the microcracks was predominantly along the tensile axis. By vacuum annealing the tensile specimens above 400°C the microcracks could subsequently be removed. However, annealing at 300°C did not remove the cracks. The process involved in microcrack annealing was found to have an activation energy of about half the value for bulk diffusion. Therefore, it appears that surface and grain boundary diffusion are the rate-controlling processes.

The microcracking reduces the fracture strength of the polycrystalline material. In principle, microcracking can also be produced by radiation-induced growth or swelling and possibly by irradiation creep.

The experimental findings by Turner et al. then imply that the combined strains produced by swelling and plastic deformation below about 350°C should not exceed about 1% if no strength degradation can be tolerated.

9. CONCLUSIONS

The radiation-induced dimensional changes in beryllium subject to a fast neutron flux are dominated by helium bubble swelling. Based on the analysis of the dislocation bias, void swelling is not expected to occur. However, the anisotropy of the dislocation structure in beryllium together with the dependence of the bias on the crystallographic orientation of the dislocation implies that bubble swelling is not isotropic within one grain. This microscopic radiation-induced growth will eventually lead to microcracking which is observed also after low-temperature plastic deformation. As a conservative design measure, it is recommended that the total inelastic strains in a beryllium structure should not significantly exceed about 1%, for temperatures below 350°C. Larger strains may be tolerated at higher temperatures.

ACKNOWLEDGEMENTS

This research has been supported in part by the Office of Fusion Energy, Department of Energy, under contract DE-AC02-82ER52082 with the University of Wisconsin, and by the Lawrence Livermore National Laboratory.

REFERENCES

1. R.D. WATSON, M.F. SMITH, J.B. WHITLEY, J.M. MCDONALD, "Thermomechanical Testing of Beryllium for the JET/ISX-B Beryllium Limiter Experiment," Proc. 13th Symp. Fusion Tech., Sept. 1984, Varese, Italy.

2. D.J. HUGHES, R.B. SCHWARTZ, BNL-325, U.S.A.E.C. (1958).

3. J.D. LEE et al., "Feasibility Study of a Fission-Suppressed Tandem Mirror Hybrid Reactor," UCID-19327, Lawrence Livermore National Laboratory (1982).

4. J.M. BEESTON, M.R. MARTIN, C.R. BRINKMAN, G.E. KORTH, W.C. FRANCIS, in Symp. on Materials Performance in Operating Nuclear Systems, CONF-73081, Ames Laboratory, Ames, IA, Aug. 1978, Nuclear Metallurgy, 19, 59-87.

5. T.E. MITCHELL, G. DAS, E.A. KENIK, "Determination of Threshold Displacement Energies by HVEM," in Fund. Aspects of Rad. Damage in Metals, Proc. Intern. Conf., CONF-751006-P1, Gatlinburg, TN, 1975, p. 73.

6. M.T. ROBINSON, "The Dependence of Radiation Effects on the Primary Recoil Energy," in "Radiation-Induced Voids in Metals," Proc. Intern. Conf., eds. J.W. Corbett and L.C. Ianniello, Albany, April 1972, p. 397.

7. J. DELAPLACE, J. HILLAIRET, J.C. NICOUD, D. SCHUMACHER, G. VOGL, Phys. Stat. Sol., 29, 819 (1968).

8. J.R. BEELER, JR., Radiation Effects Computer Experiments, North-Holland, Amsterdam (1983), p. 478.

9. J.M. DUPOUY, J. MATHIE, Y. ADDA, Mem. Sci. Rev. Met., 63, 481 (1966).

10. J.J. BURTON, Phys. Rev., B5, 2948 (1972).

11. T.A. MYERS, "The Calculation of Point and Planar Defect Formation Energies in Beryllium," in Beryllium 1977, Proc. 4th Intern. Conf. on Beryllium, The Royal Soc. London, paper 3.

12. B.B. GLASGOW, W.G. WOLFER, J. Nucl. Matls., 122 & 123, 503 (1984).

13. M. BASKES, H.H. HOLBROOK, Phys. Rev., B17, 422 (1978).

14. R.S. BARNES, G.B. REDDING, Nuclear Energy, 10, 22 (1959).

15. J.B. RICK, G.B. REDDING, R.S. BARNES, J. Nucl. Matls., 1, 73 (1959).

16. L.E. MUIR, Interfacial Phenomena in Metals and Alloys, Addison-Wesley, Redding, MA (1975), p. 124.

17. C.H. WOO, U. GOESELE, J. Nucl. Matls., 119, 219 (1983).

18. G.J.C. CARPENTER, R.G. FLECK, "Electron Irradiation Damage in Beryllium in a High-Voltage Electron Microscope," in Beryllium 1977, Proc. 4th Intern. Conf. on Beryllium, The Royal Soc. London, paper 26.

19. R.V. HESKETH, in Proc. Intern. Conf. on Sol. St. Phys. Research with Accelerators, BNL-50083(C-52) (Physics-TID-4500), Brookhaven National Lab., Sept. 1967, p. 389.

20. G.I. TURNER, R.A. LANE, R.A. LANCASTER, "On the Occurrence and Removal by Thermal Treatment of Microcracking Arising During the Uniaxial Tensile Deformation of High Purity Beryllium," in Beryllium 1977, Proc. 4th Intern. Conf. on Beryllium, The Royal Soc. London, paper 12.